The Determination of the Surface Stress in an Atmospheric Model

PETER A. E. M. JANSSEN

Department of Oceanography, Royal Netherlands Meteorological Institute (KNMI), De Bilt, The Netherlands

ANTON C. M. BELJAARS, ADRIAN SIMMONS, AND PEDRO VITERBO

European Centre for Medium-Range Weather Forecasts, Reading, Berkshire, United Kingdom

(Manuscript received 15 November 1991, in final form 23 March 1992)

ABSTRACT

By forcing a third-generation wave-prediction model with surface stresses from the European Centre for Medium-Range Weather Forecasts (ECMWF) atmospheric model, it was discovered that lower wave heights were generated than by forcing with the ECMWF surface winds. The apparent inconsistency between surface stresses and surface winds in the atmospheric model turns out to be time-step dependent. A similar conclusion may be inferred from results of the WAMDI group.

Apparently, a number of atmospheric models have inaccuracies in the boundary-layer scheme near the surface. In this paper it is argued that the reason for the inaccuracies is related to the numerical integration scheme that is used in these models. It is shown that a numerical scheme that treats physics and dynamics separately has an equilibrium that is time-step dependent. An alternative scheme—namely, simultaneous, implicit treatment of both physics and dynamics—removes this deficiency. Possible consequences for atmospheric-, wave-, and ocean-circulation models are briefly discussed.

1. Introduction

The stress in the surface layer plays an important role in a number of processes that occur at the interface of air and water or land. It not only determines to some extent the decay of a depression but it is also an important factor in the transfer of heat and moisture, a process that might deepen a depression. In addition, the stress generates ocean waves and drives the ocean circulation.

Therefore, a reliable estimation of heat and moisture fluxes, wave heights, and ocean currents requires a proper determination of the stress in the surface layer of an atmospheric model. We have evidence, however, that a number of atmospheric models determine the stress and wind speed incorrectly. This conclusion may be drawn from two experiments done by the WAMDI group (1988) with the third-generation wave model WAM.[1] In the first experiment the WAM model was forced by stresses obtained from the atmospheric model of Atlas et al. (1987), while in the second experiment surface stresses were obtained from the corresponding surface winds using a neutral drag coefficient, which is wind-speed dependent. By comparing the climatological wave-height fields obtained from a 1-month hindcast, significant differences between the two hindcasts were found: the hindcast using surface winds gave higher wave height.

A similar conclusion may be drawn from the work of Zambresky (1986). Here analyzed wind fields and 6-hour-averaged stresses from the European Centre for Medium-Range Forecasts' (ECMWF) atmospheric model were compared, the wind speed having been converted to stresses using a neutral drag coefficient from Wu (1982). Although there was some resemblance between the model stress fields and the stress fields obtained from the wind speed, maxima in the model stress fields were too low, producing again wave height that was too low.

Apparently, a number of atmospheric models have an inconsistency between the stress and the surface wind, especially when the wind speed is large. For steady flow, however, such an inconsistency should not happen, because the numerical model would violate the observed relation between wind speed and momentum loss in the surface layer. Today, it is customary to treat the turbulent diffusion in the surface layer by means of an implicit integration scheme in time (Richtmeyer and Morton 1967) because the typical relaxation time of the diffusion τ_d may be shorter than

[1] The WAM model is a wave prediction model that is based on an explicit description of the physical processes governing wave evolution, including wave–wave interactions. It was developed by a group of mainly European scientists who call themselves the WAM group.

Corresponding author address: Dr. Peter A. E. M. Janssen, ECMWF, Shinfield Park, Reading, Berkshire RG2 9AX, England.

the integration time step of the dynamical processes in the atmospheric model. As a matter of fact, the higher the wind speed, the shorter τ_d, so that for high wind speed an implicit treatment of tendencies is certainly needed in order to avoid numerical instability.

In this paper it is argued that the Richtmeyer and Morton implicit method is applied incorrectly to the evolution equations of the atmosphere. It is common practice to obtain the evolution in time of the velocity, for example, by means of the so-called time-split method. In this method, the total tendency of the wind is obtained by adding the tendencies due to dynamics (e.g., pressure and Coriolis force) and due to physics (e.g., turbulent transport of heat, moisture, and momentum). The problem is, however, that the dynamics tendency and physics tendency are obtained by different numerical schemes (e.g., Eulerian versus implicit) and then just added to give the total tendency, disregarding any possible interaction between the two. The result is a time-step-dependent equilibrium and a numerical drag coefficient that is too low for high wind speed. When, however, we treat the physical and dynamical processes on the same footing, thereby respecting possible interactions, the proper equilibrium wind speed, stress, and therefore drag coefficient are found.

The program of this paper is therefore as follows. We illustrate our idea in section 2 by considering a simple evolution equation for the average velocity in the surface layer. In section 3, the resulting numerical schemes are solved for a special case, and results are discussed. We apply in section 4 the improved numerical scheme to the equations of velocity, temperature, and moisture of a new version of the ECMWF atmospheric model at T106 resolution, and we compare for a time step of 15 min results with the time-split method. As a reference, we use a run of the model with a small time step of 1 min. Consequences for medium-range weather forecasting are discussed.

2. Integration schemes for the surface-layer equations

The purpose of this section is to discuss our idea that the time-split method gives a time-step-dependent equilibrium, while an implicit method, properly applied, results in an equilibrium solution that does not depend on time step. For illustrative purposes, we apply the two numerical schemes to a simple evolution equation for the average velocity in the surface layer with given stress at the top of the surface layer. In addition, for simplicity, we take a constant drag coefficient.

Consider the momentum balance for the horizontal components u and v of the velocity

$$\frac{\partial}{\partial t} u = -\frac{1}{\rho}\frac{\partial}{\partial x} p + fv + \frac{\partial}{\partial z}\tau_x - A_x,$$

$$\frac{\partial}{\partial t} v = -\frac{1}{\rho}\frac{\partial}{\partial y} p - fu + \frac{\partial}{\partial z}\tau_y - A_y, \qquad (1)$$

where p is the air pressure, ρ the air density, f the Coriolis parameter, τ the turbulent kinematic momentum flux, and A the advection. Integration over height z from the surface to the surface-layer height L, gives, with

$$U \equiv \frac{1}{L}\int_o^L dzu, \quad V \equiv \frac{1}{L}\int_o^L dzv,$$

the following balance equations:

$$\frac{\partial}{\partial t} U = \frac{\tau_x(L) - \tau_x(0)}{L} - \frac{1}{\rho}\frac{\partial}{\partial x} p + fV - \bar{A}_x,$$

$$\frac{\partial}{\partial t} V = \frac{\tau_y(L) - \tau_y(0)}{L} - \frac{1}{\rho}\frac{\partial}{\partial y} p - fU - \bar{A}_y, \qquad (2)$$

where an overbar means average over height. Here we assumed that the surface-layer height is so small that the height dependence of the pressure can be ignored. We will study some properties of (2) using as surface stress

$$\tau(0) = C_D|\mathbf{U}|\mathbf{U}, \qquad (3)$$

where the drag coefficient C_D is a constant and assuming that the stress at the top of the surface layer is given.

Denoting the total stress at the top of the surface layer by τ, we have

$$\tau = [\tau_x^2(L) + \tau_y^2(L)]^{1/2}. \qquad (4)$$

Then, the introduction of the dimensionless speeds

$$U' = U(C_D/\tau)^{1/2}, \quad V' = V(C_D/\tau)^{1/2}, \qquad (5)$$

and the dimensionless time

$$t' = t/\tau_d, \qquad (6)$$

where τ_d is a typical relaxation time related to, for example, turbulent momentum diffusion,

$$\tau_d = L/(C_D\tau)^{1/2}, \qquad (7)$$

gives the following evolution equations for the dimensionless velocities U and V

$$\frac{\partial}{\partial t} U = \tau_x - U(U^2 + V^2)^{1/2} - \frac{L}{\tau\rho}\frac{\partial}{\partial x} p + \omega V - \frac{L}{\tau}\bar{A}_x,$$

$$\frac{\partial}{\partial t} V = \tau_y - V(U^2 + V^2)^{1/2} - \frac{L}{\tau\rho}\frac{\partial}{\partial y} p - \omega U - \frac{L}{\tau}\bar{A}_y, \qquad (8)$$

where we dropped the primes. Here $\omega = f\tau_d$, and τ_x and τ_y are stresses at the top of the layer normalized with the total stress τ. We shall choose the stresses τ_x and τ_y in accordance with the usual relations in the Ekman layer between geostrophic wind and the mean wind of the surface layer with height L.

The need for an implicit numerical scheme to determine the evolution in time of the velocity becomes evident when the order of magnitude of the relaxation time τ_d is estimated. As an example, we take a 30-m wind speed of 25 m s^{-1}. At sea the roughness length z_o is given by the Charnock (1955) relation $z_o = \alpha\tau/g$, with $\alpha = 0.0185$ and g the acceleration of gravity. Using a logarithmic wind profile with von Kármán constant $k = 0.40$, this gives a stress $\tau = 1.09$ m^2 s^{-2} and a drag coefficient $C_D = 1.74 \times 10^{-3}$ resulting with a surface-layer height of 80 m in a relaxation time $\tau_d \approx 1800$ s, which is of the same order of magnitude as the integration time step for the physics tendencies in the T106 version of the ECMWF atmospheric model. It should be noted that over land, where the roughness length z_o is substantially larger (giving, for the same wind speed, a larger stress τ), relaxation times are even shorter.

Let us now first discuss a numerical integration scheme that gives the proper equilibrium wind speed and surface stress. To that end, we introduce the shorthand notation,

$$D_x \equiv -\frac{L}{\rho\tau}\frac{\partial}{\partial x}p + \omega V - \frac{L\bar{A}_x}{\tau},$$

$$D_y \equiv -\frac{L}{\rho\tau}\frac{\partial}{\partial y}p - \omega U - \frac{L\bar{A}_y}{\tau}, \qquad (9)$$

for the dynamics, and we denote the time level by the index n.

Keeping the contribution of advection fixed, the only nonlinear term is the one related to the turbulent momentum transport. Following Richtmeyer and Morton (1967), we therefore write

$$U|\mathbf{U}| = [\alpha U_{n+1} + (1-\alpha)U_n]|\mathbf{U}_n|, \qquad (10)$$

where in ECMWF's model $\alpha = 1.5$, and $|\mathbf{U}_n| = (U_n^2 + V_n^2)^{1/2}$ is the wind speed. With simultaneous integration of diffusion and dynamics, one obtains from Eq. (8) the following numerical scheme

$$U_{n+1} = U_n + \frac{\Delta t}{N}(\tau_x - U_n|\mathbf{U}_n| + D_{x,n}),$$

$$V_{n+1} = V_n + \frac{\Delta t}{N}(\tau_y - V_n|\mathbf{U}_n| + D_{y,n}), \qquad (11)$$

where $N = 1 + \alpha\Delta t|\mathbf{U}_n|$, and Δt the time step. It should be noted that the surface stress is given by

$$\tau_s = [\tau_x^2(0) + \tau_y^2(0)]^{1/2}, \qquad (12)$$

where

$$\tau_x(0) = [\alpha U_{n+1} + (1-\alpha)U_n]|\mathbf{U}_n|,$$

$$\tau_y(0) = [\alpha V_{n+1} + (1-\alpha)V_n]|\mathbf{U}_n|.$$

Introducing the physics tendency $\Delta\mathbf{U}_P$ and the dynamics tendency $\Delta\mathbf{U}_D$, where

$$\Delta\mathbf{U}_P = \frac{\Delta t}{N}(\boldsymbol{\tau} - |\mathbf{U}_n|\mathbf{U}_n)$$

$$\Delta\mathbf{U}_D = \frac{\Delta t}{N}\mathbf{D}_n, \qquad (13)$$

Eq. (11) may be written as

$$\mathbf{U}_{n+1} = \mathbf{U}_n + \Delta\mathbf{U}_P + \Delta\mathbf{U}_D. \qquad (14)$$

On the other hand, the time-split method treats physics and dynamics by a different numerical scheme after which the respective tendencies are just added. For small enough time steps, the dynamics tendency may be obtained with an explicit scheme; thus,

$$\Delta\mathbf{U}_D = \Delta t\mathbf{D}_n, \qquad (15)$$

while, since the integration time step might be larger than τ_d, the physics tendency is obtained by means of an implicit scheme, [cf. Eq. (13)],

$$\Delta\mathbf{U}_P = \frac{\Delta t}{N}(\boldsymbol{\tau} - |\mathbf{U}_n|\mathbf{U}_n). \qquad (16)$$

The time-split method therefore results in Eq. (14), with tendencies $\Delta\mathbf{U}_D$ and $\Delta\mathbf{U}_p$ as given in Eqs. (15) and (16). The surface stress is determined as follows. Introduce

$$\tilde{\mathbf{U}}_{n+1} = \mathbf{U}_n + \Delta\mathbf{U}_P;$$

then the stress is given by Eq. (12) with $\mathbf{U}_{n+1}$, however, replaced by $\tilde{\mathbf{U}}_{n+1}$.

The difference between the implicit method [Eqs. (13)–(14)] and the time-split method [Eqs. (14)–(16)] is now clearly related to the different treatment of the dynamics [cf. Eq. (13) with Eq. (15)]. Let us study therefore consequences for equilibria of the numerical schemes. In the steady state $\mathbf{U}_{n+1} = \mathbf{U}_n$; hence,

$$\Delta\mathbf{U}_P + \Delta\mathbf{U}_D = 0.$$

The time-split scheme then results in the condition

$$\boldsymbol{\tau} - |\mathbf{U}_n|\mathbf{U}_n = -\mathbf{D}_n(1 + \alpha\Delta t|\mathbf{U}_n|), \qquad (17)$$

from which we immediately conclude that the equilibrium is time-step dependent. In other words, in the surface layer, the effect of dynamics is considerably enhanced since Δt might be larger than 1.

Evidently, the time-split method scheme gives the wrong steady state. On the other hand, the implicit scheme results in the following equilibrium condition,

$$\boldsymbol{\tau} - |\mathbf{U}_n|\mathbf{U}_n = -\mathbf{D}_n, \qquad (18)$$

which is independent of the time step and which gives the proper steady state.

To summarize, we emphasize that the use of a time-split method for solving the surface-layer equation is not desirable because the equilibria are time-step dependent. In the next section, we discuss the differences between the two numerical schemes for the special case of a depression in the Northern Hemisphere.

3. A special case

The objection against the reasoning in section 2 may be raised that the time-step dependence of equilibria obtained from the time-split method is harmless because in the surface layer the order of magnitude of $\mathbf{D}_n$ should be small. Obviously, close to the surface the dynamics term $\mathbf{D}_n$ is not of the same order of magnitude as the stress τ (although the contribution due to advection might be considerable in mountainous areas), but it may be important enough to give rise to considerable deviations from the proper equilibrium. For this reason, we shall study the special case of a depression in the Northern Hemisphere. Therefore, we applied the time-split method [Eq. (14) with tendencies (15) and (16)] and the implicit scheme [Eq. (14) with tendencies (13)] to a depression located at 45°N; hence, the Coriolis parameter $f = 10^{-4}\,\mathrm{s}^{-1}$.

The surface-layer height was chosen in such a way that the mean wind speed corresponds to a speed at a height of 30 m; hence, for a neutrally stable flow, $L = 30e \approx 81.55$ m. The radial pressure gradient was estimated as follows. For given stress at the top of the layer, we estimate the geostrophic wind U_G using the following empirical drag law (Tennekes 1972),

$$U_G = \frac{u_*}{\kappa}\left[\log\left(\frac{\kappa u_*}{f z_o}\right) - B\right],$$

where $B = 0.92$ has been selected, κ is the von Kármán constant, and $u_* = \tau^{1/2}$, the friction velocity. As estimate of the roughness length, we used $z_o = \alpha\tau/g$ (with $\alpha = 0.0185$). The radial pressure gradient now follows from the momentum balance of Coriolis force, centrifugal force, and pressure gradient, evaluated at 500 km from the center of the low. The pressure gradient is taken to be independent of height. In addition, we assumed that at the height L there is, due to Ekman turning, some cross-isobar flow (under an angle of 20°); hence, the radial and azimuthal components of the stress at height L are given as

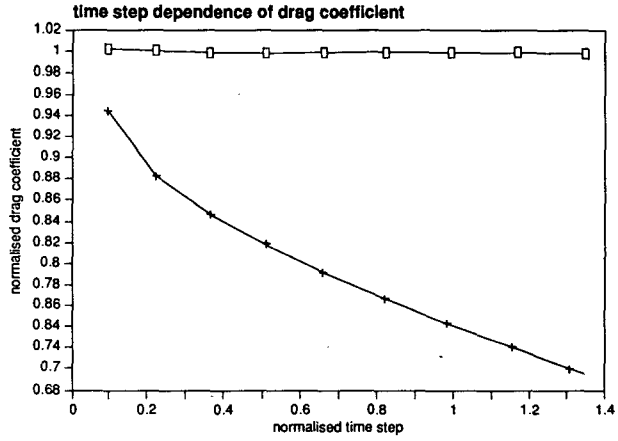

FIG. 1. Time-step dependence of drag coefficient in time split (+) and implicit scheme (□).

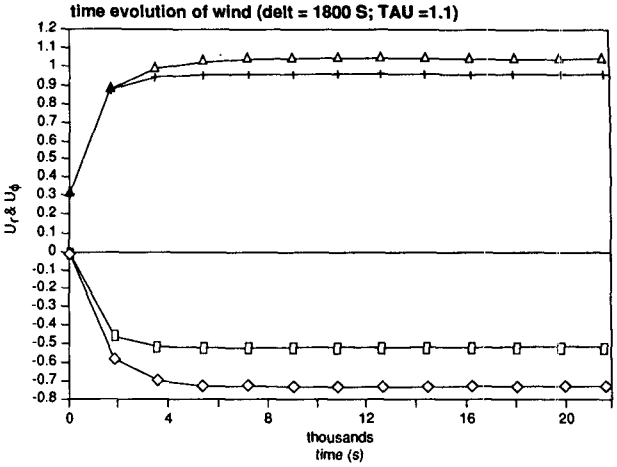

FIG. 2. Evolution in time of radial and azimuthal component of wind for time split (◇, △) and implicit scheme (□, +). Time step is 1800 s and the kinematic stress τ at height $L = 81.55$ m is 1.1.

$$\tau_r^1 = -0.35,$$

$$\tau_\phi^1 = 0.94.$$

The fixed contribution to advection was, for simplicity, given only by the centrifugal force determined by the mean wind speed in the surface layer. A time step of 1800 s was taken, which is the time step for physics in the T106 version of the ECMWF model.

In order to compare the numerical schemes, we utilized the surface stress τ_s as obtained by the two schemes; hence, for the time-split scheme we used for τ_s Eq. (12) with U_{n+1} replaced by $\tilde{U}_{n+1}$, while for the implicit scheme we used Eq. (12). The time-step dependence of the equilibria obtained by means of the time-split scheme is clearly illustrated in Fig. 1, where we have plotted the drag coefficient $C_D = \tau_s/U^2$, normalized with its proper equilibrium value (which is a given constant), as a function of the normalized time step $\Delta t/\tau_d$. The time-split scheme shows a considerable reduction of C_D of about 30% when $\Delta t/\tau_d = O(1)$, while the implicit scheme gives the proper equilibrium value of the drag coefficient.

Figure 2 shows the evolution in time of the radial and azimuthal component of the velocity according to the two numerical schemes for $\Delta t/\tau_d = 0.99$. It is clear that the time-split scheme gives too much turning of the wind in the surface layer, while the magnitude of the wind speed is too large. As a reference, we have shown in Fig. 3 the time evolution of the wind according to both schemes, but now for a time step $\Delta t = 60$ s. Both schemes are now in agreement with each other, and there is a perfect match with the results of the implicit scheme with $\Delta t = 1800$ s.

From this simple example, it is clear that the time-split method for integrating the equations of numerical weather prediction (NWP) produces inaccurate results. The same remark applies even more to climate models based on NWP models, since the normalized time step

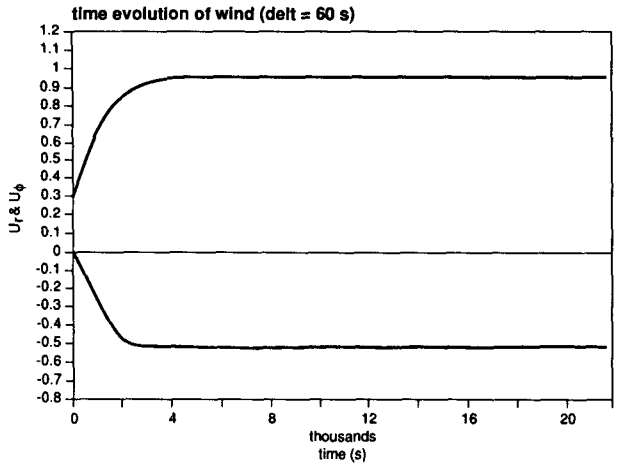

FIG. 3. Time evolution of wind velocity, but now for a time step of 1 min.

is even larger because of the larger integration time step made possible by use of lower horizontal resolution.

Finally, it is remarked that NWP models with a time-split method show a reduced sensitivity to changes in the drag coefficient. Suppose that one would like to investigate the effect of roughness on the decay of a depression. Normally, one would then increase the drag coefficient by a factor of 2, for example, and one would run the NWP model to see the effect on the pressure field. To see what really happens, we repeated the experiment with $\Delta t/\tau_d = 0.99$, and we increased the drag coefficient by a factor of 2, keeping the pressure field fixed. With the time-split method, the normalized drag coefficient was now 0.61, compared to 0.74 for the reference run, so that effectively there was an increase in drag by a factor 1.6 only.

4. Application to numerical weather prediction models

The implicit scheme has been applied to the equations for velocity, temperature, and moisture of a new version of the ECMWF atmospheric model. In previous versions the physics tendencies were obtained in gridpoint space from the equations for the components of the velocity, whereas the calculation of dynamics tendencies was only completed later in the time step, in spectral space, with the updating of the vorticity and divergence. A direct application of the implicit method was not possible in this formulation. The new version, however, produces explicit dynamical tendencies of the wind components in gridpoint space, using either an Eulerian or a semi-Lagrangian advection scheme. As physical parameterizations are evaluated at grid points immediately after this dynamical calculation, it is straightforward to include the implicit scheme in this version (Hortal 1992).

In order to show the better performance of the implicit scheme over the time-split scheme, we carried out two experiments with both schemes. The resolution was T106, 19 levels as then used operationally at ECMWF, and the Eulerian advection scheme was used. As a reference, we performed a 12-h run with an extremely small time step of 1 min, and we found that both schemes were in agreement with each other. The second experiment used a time step of 15 min, and in Figs. 4a and 4b, we have plotted the wind error of the time-split scheme and the implicit scheme, respectively, where the wind error is the difference between the 15-min time-step experiment and the reference run normalized by the results of the reference experiment. We note that these plots have been made by determining the difference vector after which the reference wind vector is turned north (keeping the angle between difference and reference wind vector fixed) and scaling it to 100%. The advantage of this convention is that it is immediately clear when there are wind-speed errors (difference vector is either pointing north or south) or differences in direction (difference vector is pointing east or west). From Fig. 4a it is observed that the time-split scheme with 15-min time step produces wind speed that is too large, while (see, for example, in the Northern Hemisphere) the cross-isobar flow is too large as well. Although there are significant differences over the oceans, the differences over land, especially in mountainous areas, are more substantial. By comparison, the differences found using the implicit scheme are insignificant; hence, use of the implicit scheme will result in wind speeds that are smaller than those produced by the time-split scheme.

Figures 5a and 5b show the instantaneous, relative stress errors for the time-split scheme and the implicit scheme. Again, model stresses are determined in the same way as in sections 2 and 3. Clearly, both schemes show significant errors, but we were unable to detect any systematic trend from these plots. Over the oceans, however, the stress errors produced by the implicit scheme are quite small. In order to see this, we have plotted in Figs. 6a, 6b, and 6c the drag coefficient C_D as a function of the lowest-level wind speed for the time-split scheme, the implicit scheme, and the 1-min time-step run, respectively. We took as area the Southern Hemisphere oceans, and we selected neutrally stable or slightly unstable cases ($0 \leqslant \mathrm{Ri} < -0.5$, where Ri is the bulk Richardson number). For near-neutral cases the drag coefficient is given by $C_{DN} = \{\kappa[\log(L/z_o)]^{-1}\}^2$ (where the roughness length is given by the Charnock relation $z_o = \alpha\tau/g$ (with $\alpha = 0.0185$)] and as a reference we have plotted C_{DN} as function of the lowest wind speed U_{31}.

The time-split scheme gives, as expected, a drag coefficient that is too low for high wind speed, and a considerable scatter is found. On the other hand, the implicit scheme (Fig. 6b) has no bias, but when compared with the small time-step run (Fig. 6c), the scatter around the neutral curve is larger. In this connection

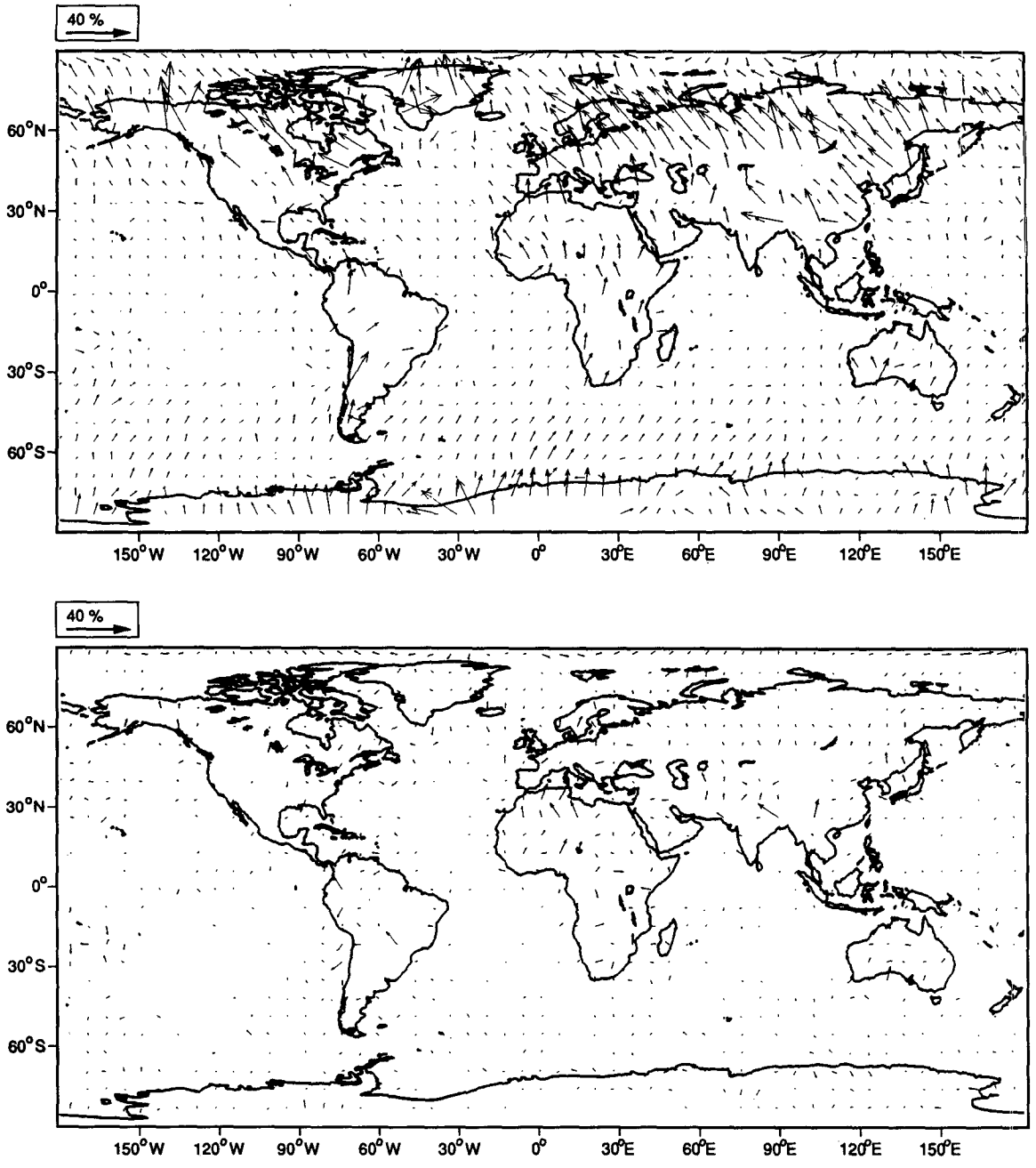

FIG. 4. Global map of wind-speed error of (a) time-split scheme and (b) implicit scheme, where the error is the difference between 15-min time-step results and 1-min time-step results.

it should be remarked that the scatter in Fig. 6b can already be explained by assuming a change in wind speed of 10% in half an hour (which is reasonable). Using Eq. (12) for the surface stress, one obtains with $U_{n+1} = (1 + \Delta)U_n$,

$$\tau_s = (1 + \Delta\alpha)U_n^2,$$

giving a relative scatter in the drag coefficient of the order of $\Delta\alpha$%. With $\Delta = 10\%$ and $\alpha = 1.5$, a scatter results that is in reasonable agreement with Fig. 6b. Thus, unsteadiness may explain the scatter in the relation between drag coefficient and wind speed for the implicit scheme with a large time step. The corresponding scatter for the 1-min time-step run, on the other hand, seems too large, and we do not understand how it is caused.

Over land, especially in mountainous areas, both schemes are very sensitive to changes in the time step (see also Klinker and Sardeshmukh 1987). As already

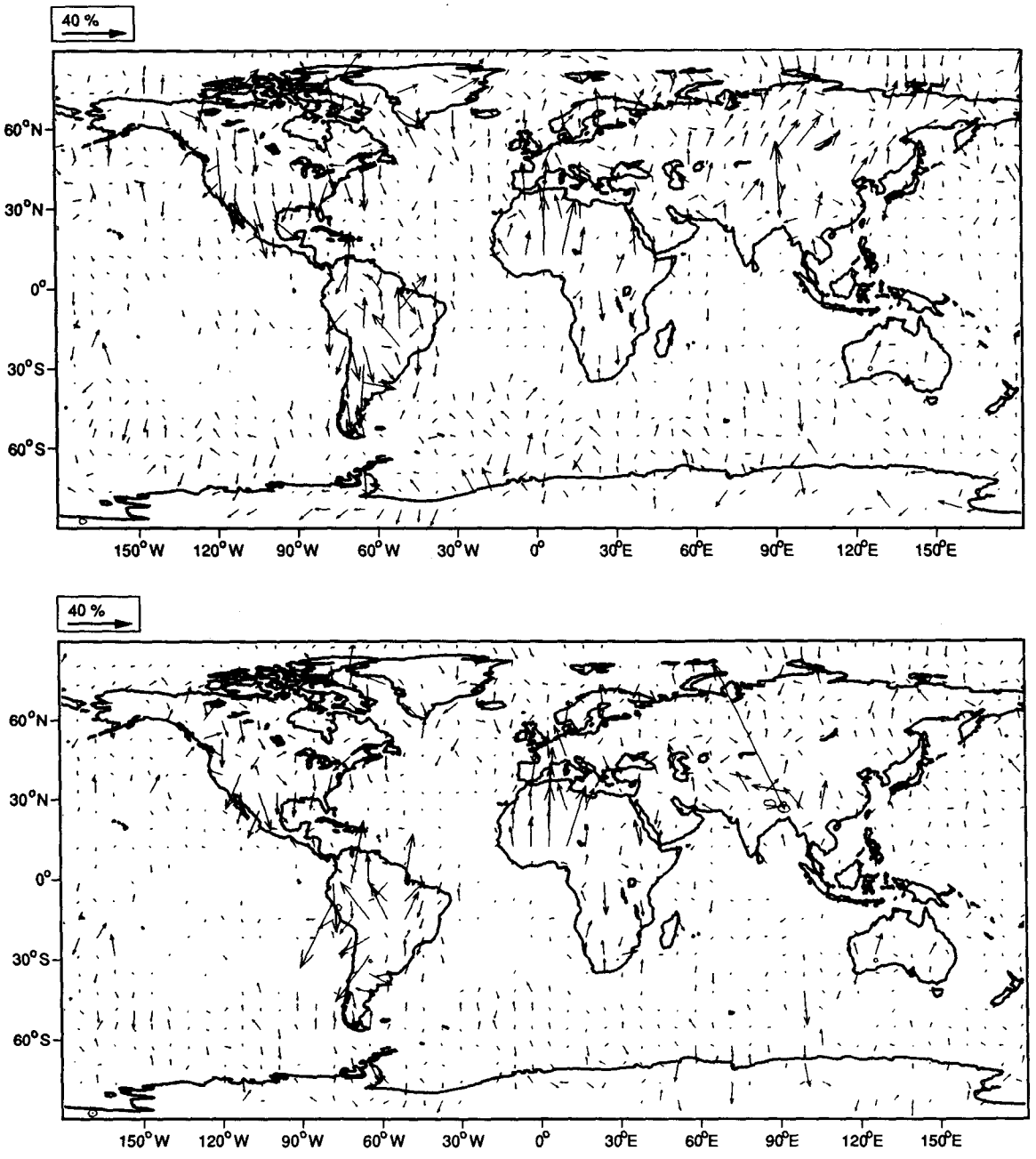

FIG. 5. Global map of instantaneous stress errors for (a) time-split scheme and (b) implicit scheme.

mentioned in the previous section, a principal reason for this is that cases of large deviation from geostrophy are not handled well by the time-split scheme, and flow over mountainous areas is an extreme example of ageostrophic flow. Furthermore, neither scheme handles time-dependent cases accurately.

It should be realized that the implicit scheme has a significant impact on the wind speed and also on the wind direction. Compared to results with the time-split scheme, a reduction in wind speed is found. Since the ECMWF model (with time-split scheme) is known to produce high-quality wind fields (Zambresky 1989), the quality of the wind fields using the implicit scheme may get worse.

Finally, we also investigated the impact of the implicit scheme on weather prediction in the medium range. Two 10-day forecasts were carried out using the semi-Lagrangian version with 31 levels and T106 resolution. Both the splitting and the implicit scheme were used with a time step of 30 min (60 min for a single physics time step because of the leapfrogging). The Northern Hemisphere anomaly correlation of the 500-

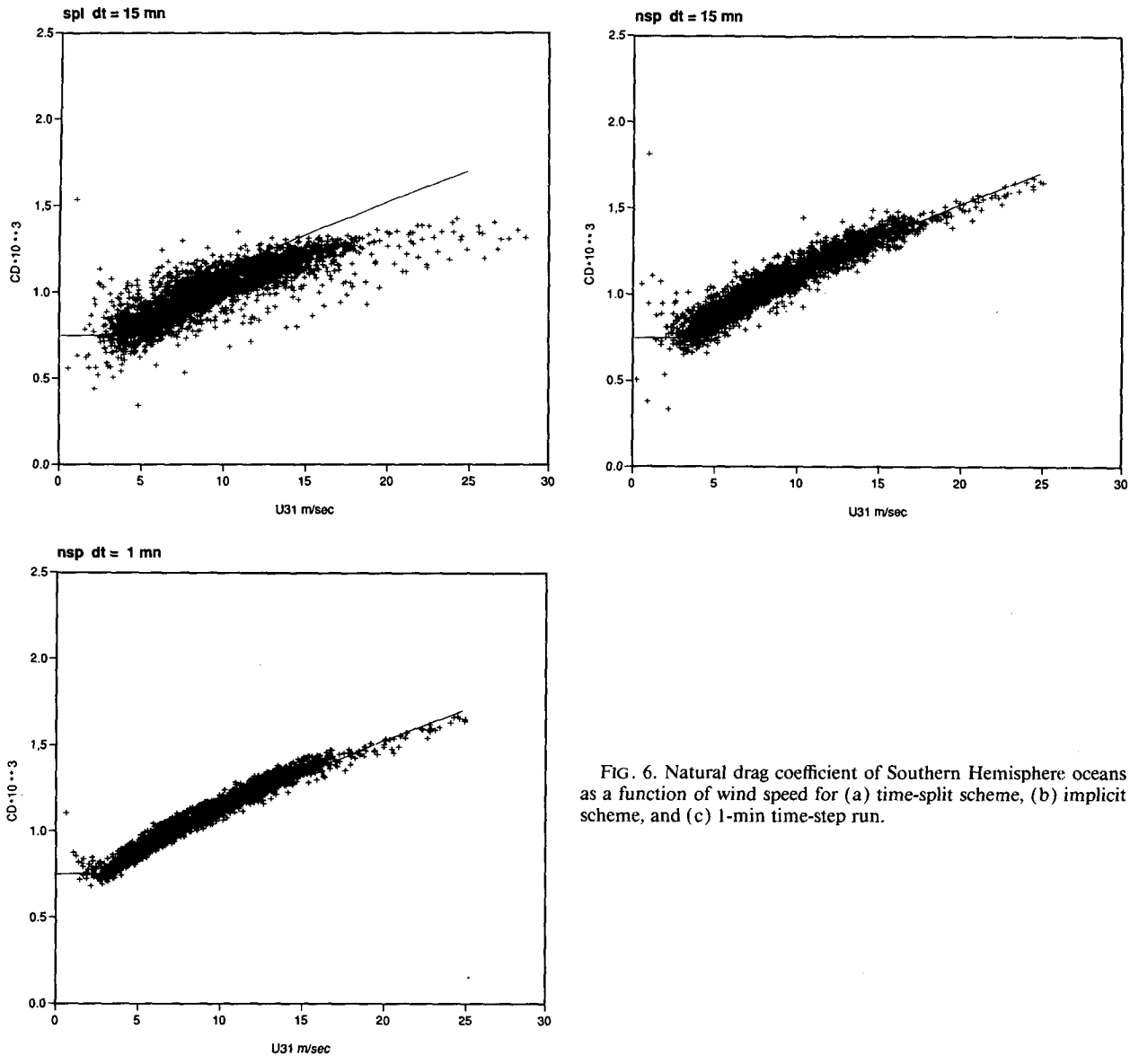

FIG. 6. Natural drag coefficient of Southern Hemisphere oceans as a function of wind speed for (a) time-split scheme, (b) implicit scheme, and (c) 1-min time-step run.

and 1000-hPa levels (see Fig. 7) shows relatively small impact from the new scheme, probably because the new scheme does not change the surface fluxes in a systematic way. The main impact is on the magnitude of the surface wind rather than on the momentum budget of the model atmosphere. Improving the quality of the surface wind by retuning the boundary-layer scheme might affect the momentum budget, however, because in the implicit scheme there is consistency between surface winds and stresses.

5. Conclusions

In this paper we have addressed the problem of the proper determination of the stress in the surface layer of numerical weather prediction models. The commonly used time-split scheme was shown to produce equilibria that are time-step dependent and, especially for high wind speed, reduce the drag coefficient.

The implicit scheme, which integrates the vertical diffusion with the dynamics tendency as source term, is shown to give the proper equilibrium wind speed and stress, independent of the time step.

It should be realized, however, that there is no guarantee that the implicit scheme is accurate in time-dependent circumstances. Although the comparison of Figs. 2 and 3 might suggest the opposite, since a good agreement between large and small time-step results is found, it should be remarked that this result depends on the choice of the surface-layer height L and the constant α. For example, for smaller L and α fixed, a large time-step run would show overshoot behavior in the time series for the wind, while the corresponding short time-step run does not show such a behavior. By

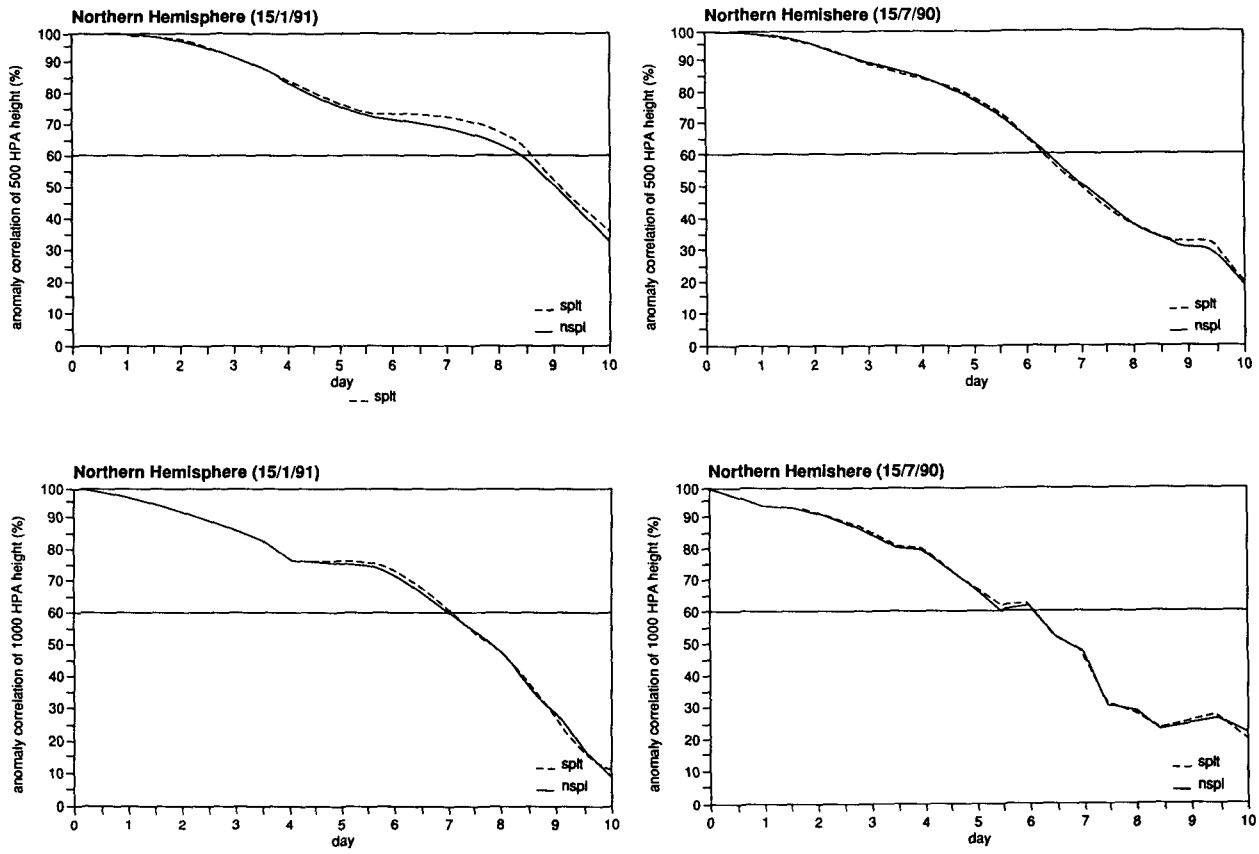

FIG. 7. Northern Hemisphere anomaly correlation of 1000- and 500-hPa height for (a) time-split and (b) implicit scheme.

increasing α, however, the overshoot behavior in the large time-step run can be suppressed. In unsteady circumstances, however, a time-step dependence still remains, as is shown in Figs. 6b and 6c.

The impact of the new scheme on the quality of medium-range weather forecasts is small, probably because the surface fluxes are hardly changed. The main impact of the new scheme is a reduction of the near-surface wind speed. The old scheme had a systematic time-step-dependent bias in the near-surface wind.

Finally, we emphasize again the relevance of an accurate stress determination for wave prediction, storm-surge modeling, and ocean-circulation modeling. In particular, the relevance of a proper integration scheme in the field of climate modeling should be pointed out, because the accuracy of the simulated transfer of momentum, heat, and moisture plays an important role in the problem of climate drift.

REFERENCES

Atlas, R., A. J. Busalachi, M. Ghil, S. Bloom, and E. Kalnay, 1987: Global surface wind and flux fields from model assimilation of SEASAT data. *J. Geophys. Res.*, **92,** 6477–6487.

Charnock, H., 1955: Wind stress on a water surface. *Quart. J. Roy. Meteor. Soc.*, **81,** 639–640.

Hortal, M., 1992: Formulation of the ECMWF model. *Proc. Seminar on Numerical Method in Atmospheric Models,* Reading, United Kingdom, ECMWF, 261–280.

Klinker, E., and P. D. Sardeshmukh, 1987: The diagnosis of systematic errors in numerical weather prediction models. *Proc., ECMWF Workshop on Diabatic Forcing,* Reading, United Kingdom, ECMWF, 209–244.

Richtmeyer, R. D., and K. W. Morton, 1967: *Difference Methods for Initial-Value Problems.* Interscience, 405 pp.

Tennekes, H., 1972: Similarity laws and scale relations in planetary boundary layers. *Workshop on Micrometeorology,* Boston, Amer. Meteor. Soc., 177–216.

WAMDI group: Hasselmann, S., K. Hasselmann, E. Bauer, P. A. E. M. Janssen, G. J. Komen, L. Bertotti, P. Lionello, A. Guillaume, V. C. Cardone, J. A. Greenwood, M. Reistad, L. Zambresky, and J. A. Ewing, 1988: The WAM model—A third generation ocean wave prediction model. *J. Phys. Oceanogr.*, **18,** 1775–1810.

Wu, J., 1982: Wind stress coefficients over sea surface from breeze to hurricane. *J. Geophys. Res.*, **87,** 9704–9706.

Zambresky, L., 1986: The WAMS project, study III. Unpublished Report, 116 pp. [Available from KNMI, P.O. Box 201, 3730 AE De Bilt, The Netherlands]

——, 1989: A verification study of the global WAM model, December 1987–November 1988. ECMWF Tech. Rep. 63, 86 pp.